

Supporting Information

Molecular-level Insights on Reactive Arrangement in On-surface Photocatalytic Coupling Reactions using Tip-enhanced Raman Spectroscopy

Zhen-Feng Cai,¹ Juan Pedro Merino,² Wei Fang,^{1,3} Naresh Kumar,^{1*} Jeremy O. Richardson,¹ Steven De Feyter,² and Renato Zenobi^{1*}

¹ Department of Chemistry and Applied Biosciences, ETH Zurich, Zurich, Switzerland.

² Department of Chemistry, Division of Molecular Imaging and Photonics, KU Leuven, Celestijnenlaan 200F, B-3001 Leuven, Belgium

³ Department of Chemistry, Fudan University, Shanghai 200438, P. R. China

Experimental Details

Sample preparation. 4-NTP and 4-ATP were purchased from Sigma-Aldrich and used without further purification. Solutions of 4-NTP/4-ATP were prepared by dissolving the solid sample in ethanol and further dilution to generate concentration series. TS-Au substrates were prepared using the procedure described in our previous work.¹ The Au(111) single-crystal substrates were prepared by the Clavilier method.² To prepare “immersion samples”, freshly prepared Au substrates were immersed in 10 mM solution of 4-NTP (or 4-ATP) in ethanol for 24 hours to allow formation of a SAM. To prepare “drop-cast samples”, 5 μ L of 10 mM 4-NTP (or 4-ATP) ethanolic solution was drop-cast onto freshly prepared Au substrates and allowed to dry naturally for *ca.* 1 min.

TERS setup. All TERS measurements were performed with a top-illumination TERS setup combining an STM with a Raman spectrometer (NTEGRA Spectra Upright, NT-MDT, Russia). A 100 \times , 0.7 NA air objective (Mitutoyo, Japan) was used for both excitation and collection of the TERS signals. STM and TERS measurements were performed using electrochemically etched Ag tips.³ A 632.8 nm He-Ne laser (Spectra-Physics, Newport, Germany) with a power of 70 μ W on the sample was used as the excitation source. For all TERS measurements, tunnelling current was set to 200 pA, tunnelling bias was set to 1.0 V and acquisition time per spectrum was set to 4 s.

STM measurements. All experiments were performed at room temperature using a PicoLE STM (Agilent, Technologies, USA) operating in constant-current mode. STM tips were prepared by mechanical cutting of Pt/Ir wire (80/20, diameter 0.25 mm, Advent Research Materials, UK). Au(111)/mica was used as the substrate for STM measurements at the air-solid interface under ambient conditions. STM parameters are indicated in the figure captions and sample bias and tunnelling current are denoted by V_{bias} and I_{set} , respectively. The bias voltage refers to the substrate. High-resolution STM images were obtained after two hours of instrument stabilization *via* continuous imaging at phenyl octane/ Au(111) interface. Distances are determined based on the STM scanner calibration file, the accuracy of which is regularly checked by

measuring the atomic lattice of highly oriented pyrolytic graphite. STM images were processed using WSxM software.⁴ Materials Studio 7.0 software was used to build DFT-based molecular models (CASTEP simulation).

DFT calculations. DFT calculations were carried out using Vienna ab-initio Simulation Package (VASP)⁵ with optB88-vdW functional⁶, which accurately accounts for van-der-Waals interactions, and has been widely used to study the adsorption of molecules on metal surfaces.⁷ The lattice parameters of a variety of solids predicted by the optB88-vdW functional are also in good agreement with the experimental lattice parameters.⁸ A plane-wave cut-off of 450 eV was used throughout. The metal surface was represented using a slab with 4 layers of Au in a $\sqrt{7}\times\sqrt{7}$ unit cell with a $7\times 7\times 1$ K-point mesh. We used a 4×4 unit cell with a $3\times 3\times 1$ K-point mesh for the investigation of the rotation of non-close-packed 4-NTP. A vacuum of at least 22 Å was placed above each surface. The bottom 3 layers of the substrate were fixed during the optimization while all the other atoms were flexible. The force convergence criteria for the geometry optimization is 0.02 eV/Å (0.04 eV/Å for the calculations in the 4×4 unit cell).

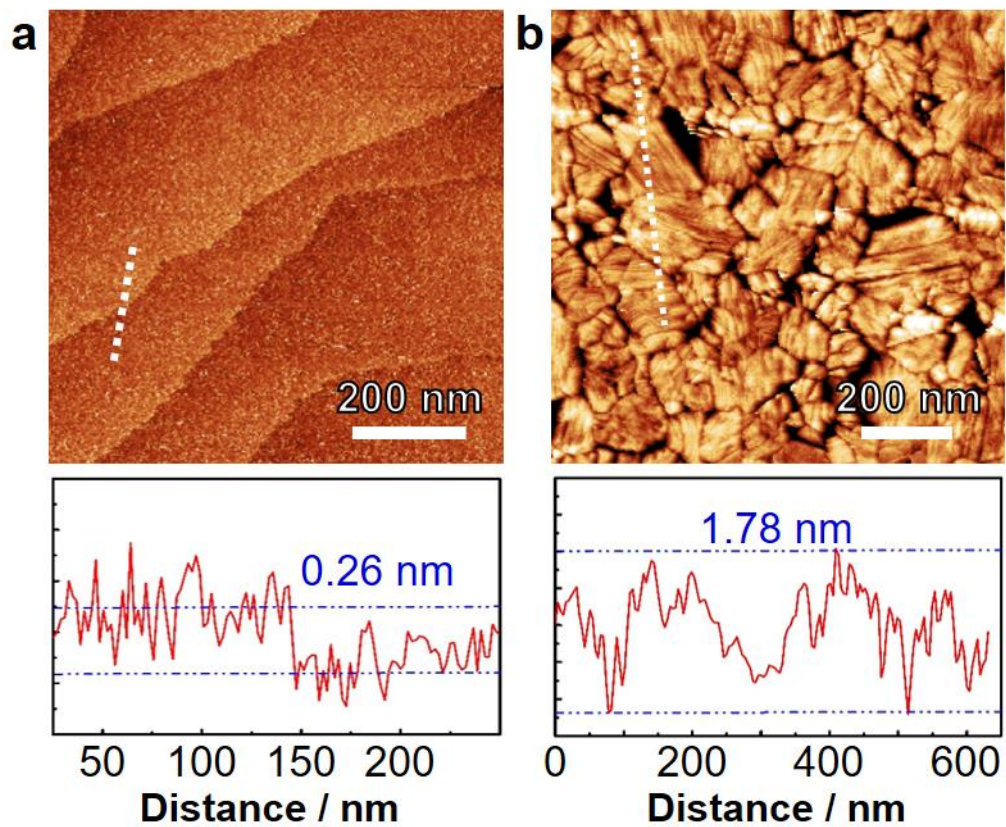


Figure S1. STM images of bare (a) Au(111) and (b) TS-Au substrates. The cross-section profiles under the STM images show topography variation along the white dashed lines marked in (a) and (b), respectively.

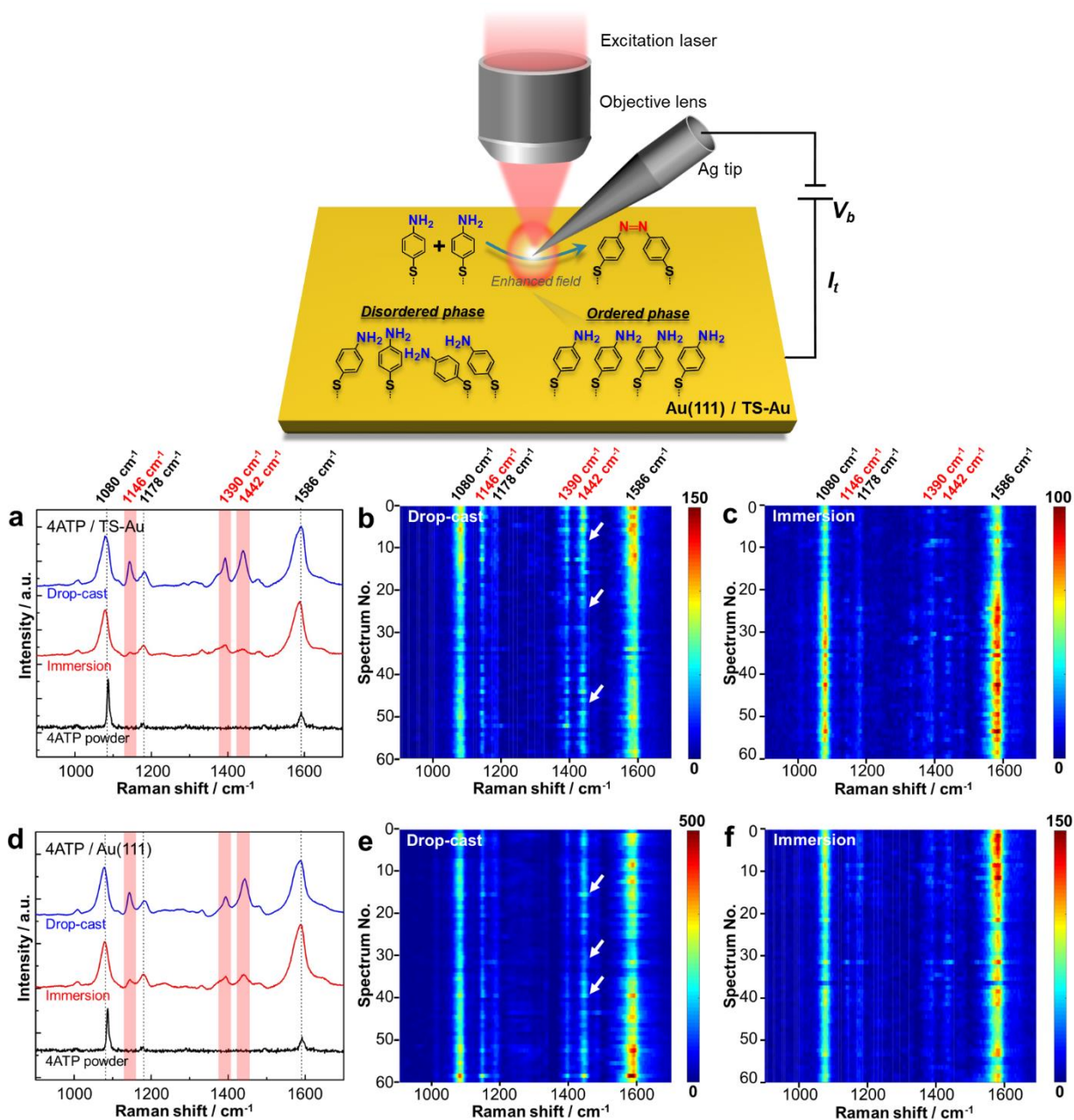
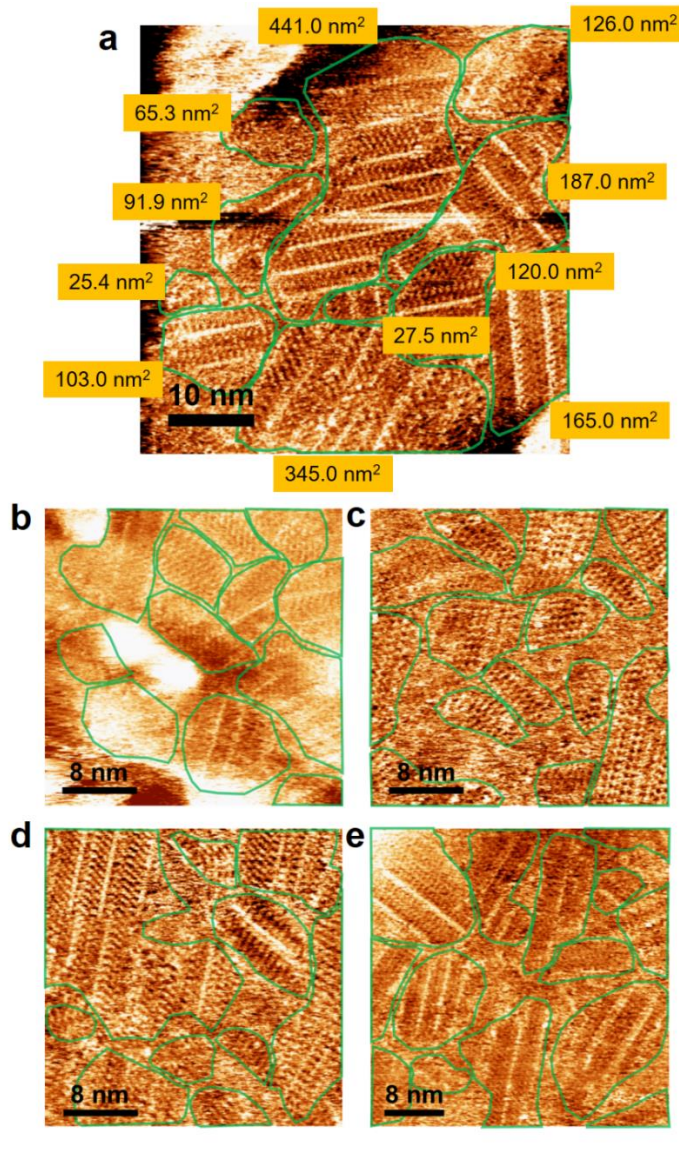


Figure S2. Top panel: Schematic diagram of the STM-TERS set up used for investigating photocatalytic coupling of 4-ATP \rightarrow DMAB on Au(111) and TS-Au surfaces. Averaged spectra measured in the TERS images (1 μm^2) of 4-ATP functionalised (a) TS-Au and (d) Au(111) surfaces prepared *via* drop-cast (blue trace) or immersion (red trace) protocols. Step size: 100 nm. Raman bands of DMAB at 1146, 1390, and 1442 cm^{-1} are highlighted in red. Raman spectrum of 4-ATP powder (black trace) is also plotted for comparison. Waterfall plots of TERS spectra measured in the TERS images of 4-ATP \rightarrow DMAB on (b, c) TS-Au and (e, f) Au(111) surfaces prepared *via* drop-cast and immersion protocols, respectively. All TERS measurements in (a- f) were performed using the same Ag probe.



	a	b	c	d	e
Area _{ordered-phase} / nm ²	1697.1	660.7	671.8	748.0	1162.3
Area _{total} / nm ²	2500	900	900	900	1600
Coverage / %	67.9	73.4	74.6	83.1	72.6

Figure S3. (a) High-resolution STM image of 4-NTP monolayer at the air/Au(111) interface presented in Figure 3a. (b) - (e) Additional high-resolution STM images of the immersion samples showing well-ordered 4-NTP domains on Au(111) surface. STM parameters: $I_t = 0.11$ nA; $V_{\text{bias}} = -0.20$ V. (f) Table listing measured area of well-ordered domains, total area of the STM image and domain coverage. Overall surface coverage of the well-ordered domains in (a) - (e) is estimated to be $74.3\% \pm 5.5\%$, where uncertainty represents image to image variation.

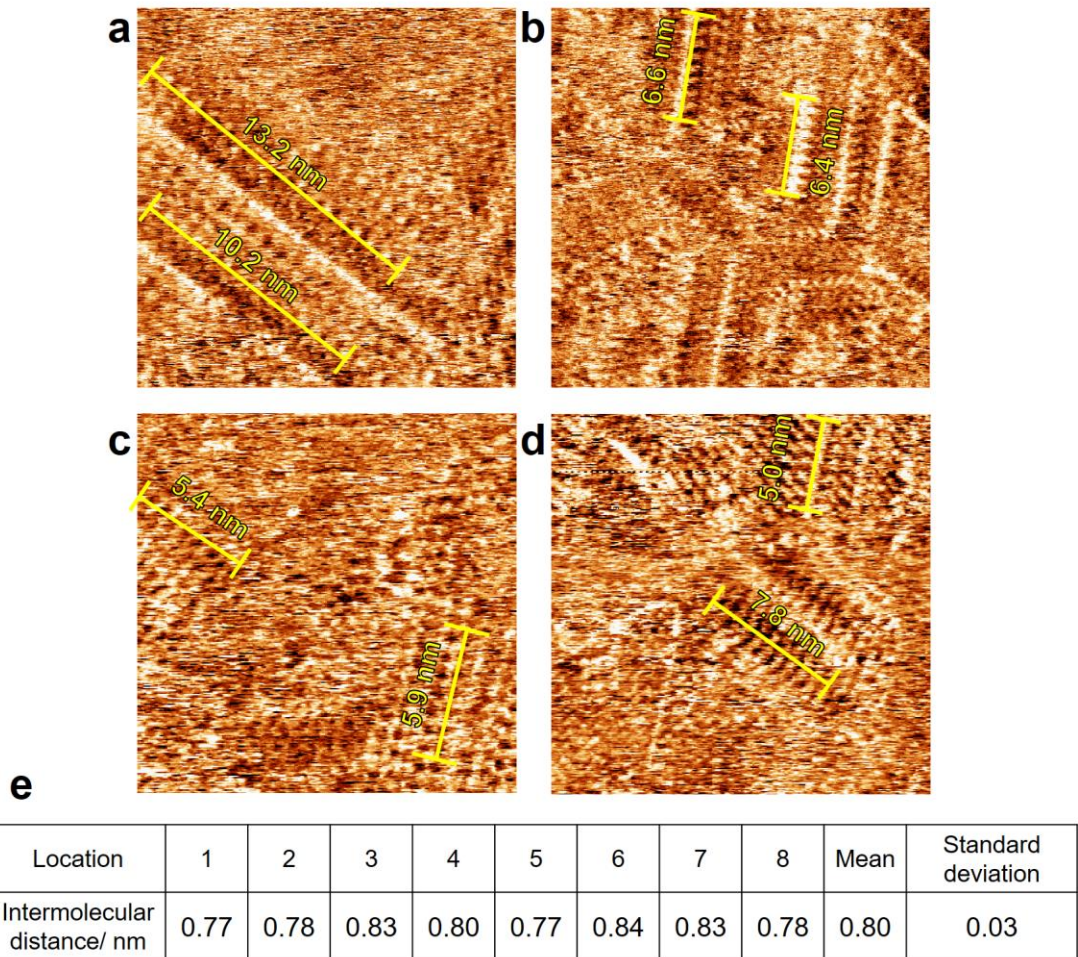


Figure S4. (a) - (d) High-resolution STM images of 4-NTP domains at air/Au(111) interface. STM parameters: $I_t = 0.11$ nA; $V_{\text{bias}} = -0.20$ V. (e) Table listing the average intermolecular distance calculated from the lines marked in (a) - (d).

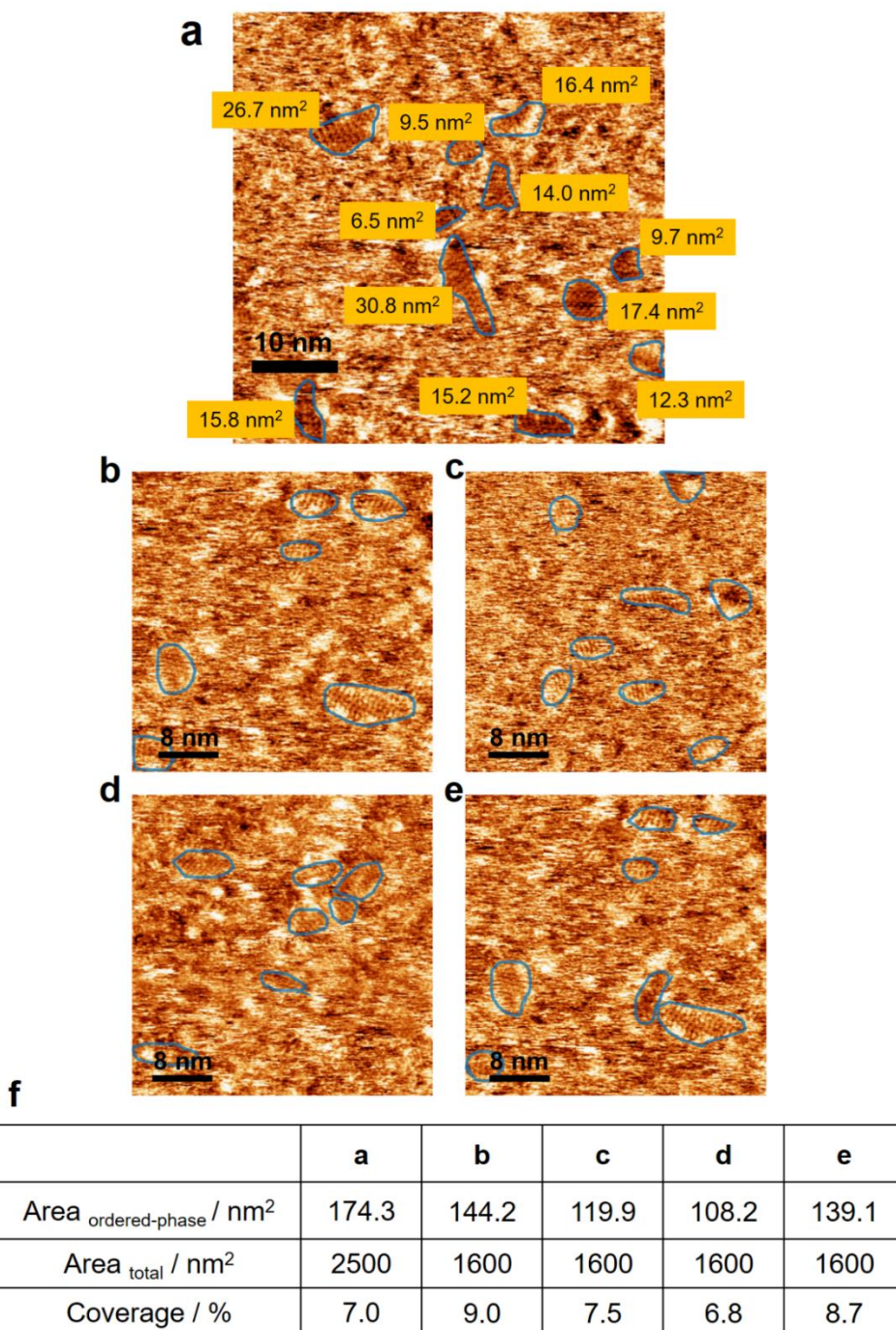


Figure S5. (a) STM image of 4-NTP monolayer at air/Au(111) interface presented in Figure 3d. (b) - (e) Additional high-resolution STM images of a drop-cast sample showing disordered 4-NTP adlayers formed on Au(111) surface. STM parameters: $I_t = 0.15$ nA; $V_{\text{bias}} = -0.20$ V. (f) Table listing measured area of well-ordered domains, total area of the STM image and domain coverage. Overall surface coverage of the well-ordered domains in (a) - (e) is estimated to be $7.8\% \pm 1.0\%$, where uncertainty represents image to image variation.

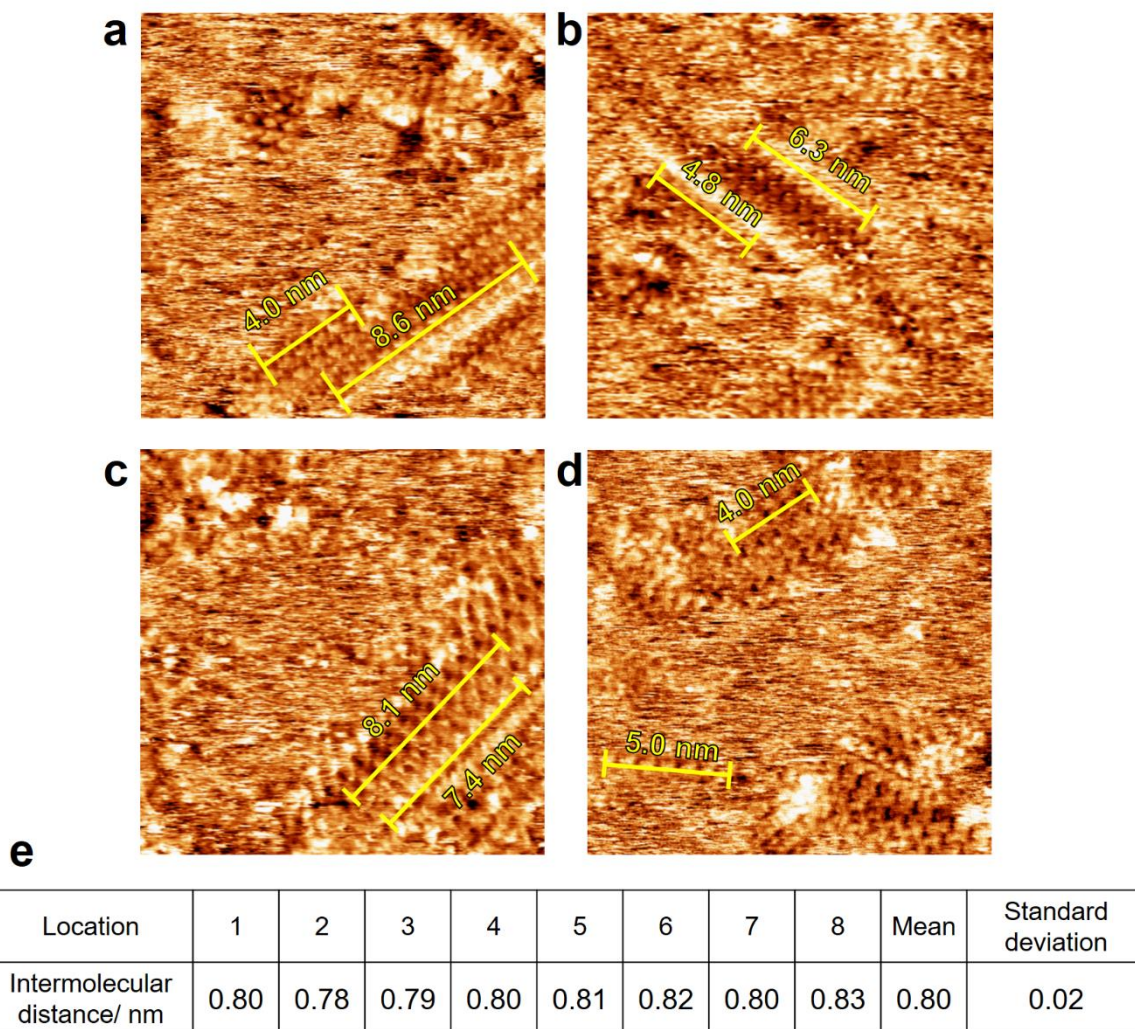


Figure S6. (a) - (d) High-resolution STM images of 4-NTP domains at air/Au(111) interface. STM parameters: $I_t = 0.15$ nA; $V_{\text{bias}} = -0.20$ V. (e) Table listing average intermolecular distance calculated from the lines marked in (a) - (d).

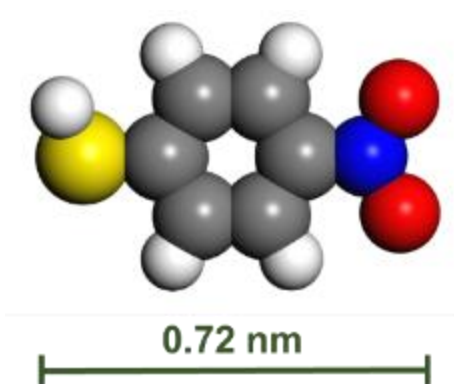


Figure S7. Optimized structural model of a 4-NTP molecule calculated using DFT. The atoms are colored as follows: H, white; C, grey; S, yellow; N, blue; O, red.

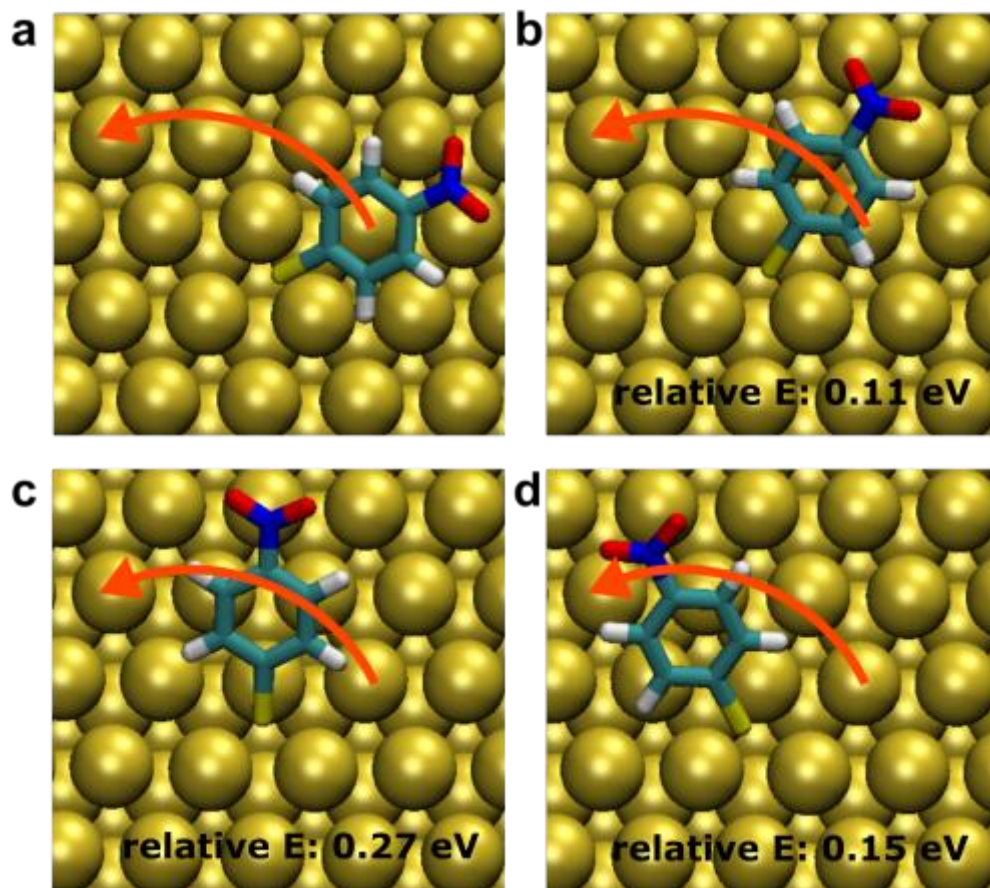


Figure S8. (a) - (d) Top view of the rotation of a 4-NTP molecule adsorbed on Au(111) in a non-close-packed adlayer calculated using DFT. The atoms are colored as follows: H, white; C, cyan; S, yellow; N, dark blue; O, red; Au, gold. The most stable adsorption of a 4-NTP molecule occurs near the FCC site.⁹ The activation energy required for the molecule to rotate around the adsorbed site to adopt a favorable configuration for $4\text{-NTP} \rightarrow \text{DMAB}$ reaction is *ca.* 0.3 eV, which corresponds to a rate on the order of ns at room temperature, assuming an attempt frequency on the order of fs. Therefore, even though it is unlikely to rotate at each attempt, it's still fast relative to the experimental timescale of 1-4 s.

Supplementary references

- (1) (a) Opilik, L.; Payamyar, P.; Szczerbiński, J.; Schütz, A. P.; Servalli, M.; Hungerland, T.; Schlüter, A. D.; Zenobi, R. Minimally Invasive Characterization of Covalent Monolayer Sheets Using Tip-Enhanced Raman Spectroscopy. *ACS Nano* **2015**, *9*, 4252. (b) Weiss, E. A.; Kaufman, G. K.; Kriebel, J. K.; Li, Z.; Schalek, R.; Whitesides, G. M. Si/SiO₂-Templated Formation of Ultraflat Metal Surfaces on Glass, Polymer, and Solder Supports: Their Use as Substrates for Self-Assembled Monolayers. *Langmuir* **2007**, *23*, 9686.
- (2) Clavilier, J.; Faure, R.; Guinet, G.; Durand, R. Preparation of monocrystalline Pt microelectrodes and electrochemical study of the plane surfaces cut in the direction of the {111} and {110} planes. *J. Electroanal. Chem. Interfacial Electrochem.* **1980**, *107*, 205.
- (3) Stadler, J.; Schmid, T.; Zenobi, R. Nanoscale Chemical Imaging Using Top-Illumination Tip-Enhanced Raman Spectroscopy. *Nano Lett.* **2010**, *10*, 4514.
- (4) Horcas, I.; Fernández, R.; Gómez-Rodríguez, J. M.; Colchero, J.; Gómez-Herrero, J.; Baro, A. M. WSXM: A software for scanning probe microscopy and a tool for nanotechnology. *Rev. Sci. Instrum.* **2007**, *78*, 013705.
- (5) Kresse, G.; Furthmüller, J. Efficient iterative schemes for ab initio total-energy calculations using a plane-wave basis set. *Phys. Rev. B* **1996**, *54*, 11169.
- (6) Klimeš, J.; Bowler, D. R.; Michaelides, A. Chemical accuracy for the van der Waals density functional. *J. Phys.: Condens. Matter* **2009**, *22*, 022201.
- (7) (a) Carrasco, J.; Klimeš, J.; Michaelides, A. The role of van der Waals forces in water adsorption on metals. *J. Chem. Phys.* **2013**, *138*, 024708. (b) Berland, K.; Cooper, V. R.; Lee, K.; Schröder, E.; Thonhauser, T.; Hyldgaard, P.; Lundqvist, B. I. van der Waals forces in density functional theory: a review of the vdW-DF method. *Rep. Prog. Phys.* **2015**, *78*, 066501.
- (8) Klimeš, J.; Bowler, D. R.; Michaelides, A. Van der Waals density functionals applied to solids. *Phys. Rev. B* **2011**, *83*, 195131.
- (9) Yin, H.; Zheng, L.-Q.; Fang, W.; Lai, Y.-H.; Porenta, N.; Goubert, G.; Zhang, H.; Su, H.-S.; Ren, B.; Richardson, J. O.; Li, J.-F.; Zenobi, R. Nanometre-scale spectroscopic visualization of catalytic sites during a hydrogenation reaction on a Pd/Au bimetallic catalyst. *Nat. Catal.* **2020**.